Quasi-steady Aerodynamic Data for Moderate Transition Icing of a Single Conductor

Dr. N. Popplewell
Department of Mechanical and Manufacturing Engineering, University of Manitoba
15 Gillson Street, Winnipeg, Manitoba, Canada, R3T 5V6

***Abstract*—Outdoor freezing rain simulations using short conductor samples support the need to introduce a transition between the traditional rime and glaze categorizations. Empirical equations are shown to reasonably describe, at different wind incidences α, a transition icing's overall aerodynamic behaviour for modest precipitations under windless conditions or with a 13 m/s side wind. The equations' simple format encourages a more universal determination of trends for power line galloping. On the other hand, maximax (over α) aerodynamic coefficients are also important for design and safety assessments. They are found to grow linearly with an increasing amount of (combined) precipitation for transition icing subject to wind. The maximax aerodynamic drag coefficient, however, grows at about twice the rate or more of the maximax lift and moment coefficients. Maximax data may be relatively unaffected by a conductor's diameter but the mean volume diameter (MVD) of a freezing rain's droplets may play a role, especially at higher precipitation amounts. Regardless, a realistic assessment of the drag should be included appropriately with the accreted ice weight in evaluating a line's safe load.**

I. Nomenclature

a_i, b_i	empirical coefficients describing the aerodynamic coefficients. The subscript indicates the lift, drag and moment coefficient corresponding to i=L, D, and M, respectively
d	water droplets' mean volume diameter, MVD
t_{max}	total time to acquire a given ice accretion
V_T	(vertical) terminal speed of a freely falling water droplet
C_D, C_L, C_M	aerodynamic drag, lift and moment coefficient respectively
D_o	conductor's diameter
H_h, H_v, H	horizontal and vertical components, respectively, of the combined precipitation amount, H
G	liquid water content of air
P=H/t_{max}	average precipitation rate
(N)R	(no) up to ±20° conductor rotation
(N)W	(no) 13 m/s side wind
α	wind's angle of incidence to conductor
$\beta=\sqrt{1+\left(\frac{H_h}{H_v}\right)^2}$	empirically determined factor relating the horizontal and vertical amounts of precipitation

II. Introduction

THERE are two primary concerns from the perspective of structural integrity when ice is accreted on an overhead power line in a freezing rainstorm. They are: (1) the weight of the accreted ice, and (2) the aerodynamic characteristics arising from the size, shape and texture of the accretion. Ice weight measurements obtained by using an outdoor freezing rain simulator [1] have been shown to correlate well with Goodwin's simple icing model [2]. On the other hand, aerodynamic data has been based on unrepresentative ice accretions or has been limited in scope. It is the aim here to suggest an aerodynamic template.

Ice accretions are categorized traditionally as either rime (dry) or glaze (wet) [3]. However, visual observations [2] for a comprehensive range of environmental conditions revealed somewhat novel ice forms in an intermediate or transition category. Then water droplets do not freeze immediately upon contacting a conductor (like rime ice) but the resulting surface water does not have the mobility of that for glaze. The main visual difference between transition and glaze icing, say, is that a continuous ice protrusion or ridge, rather than individual icicles, eventually forms beneath the conductor. Thus the appearance of a conductor's cross section becomes more like an airfoil.

An assessment of the aerodynamic nature of transition icing is presented here. This particular category is chosen because of its novelty and an associated airfoil ice shape's likely generation of severe aerodynamic behaviour.

III. Experimental details

An outdoor facility was built about 20 years ago to simulate freezing rain. Water precooled to about 2 °C supplies a uniformly distributed array of plungerless hypodermic syringes from which droplets are blown using external compressed air. The droplets fall about 7 m under gravity, becoming subcooled in the naturally cold fall or spring atmosphere, reach their terminal speed before impinging on about 1½ m long, horizontal conductor samples close to the ground. Experience indicated that the original droplet generator could be replaced with merely two nozzles. Then water droplets are sprayed into the atmosphere before they fall (about 7 m again) onto a conductor sample. Experiments are performed only when the natural wind's speed is less than 2 m/s. An essentially uniform airflow may be generated but only around the level of a conductor sample by employing a

fan coupled to a large settling chamber. The modified simulator was used to measure the ice weight accreted on different conductor samples. However, consistent results required the measurement of the horizontal as well as the vertical precipitation (H_h and H_v, respectively), especially when the fan operates. The inconsistency arose because space limitations prevented the freezing water droplets from attaining the speed of the horizontal airflow from the settling chamber before impacting the conductor sample.

Circumstances under which transition icings occurred are detailed in Table I. Both the original and modified droplet generators were used to obtain the corresponding cross sections presented in Fig. 1. Conductor designations C and TB indicate the source of the data ([4] and [5], respectively). C conductors have a nominally constant 28.6 mm diameter and two different end supports, i.e. fixed or with a possible, stop limited, ±20° rotation. Both conditions represent transmission line positions at or near a span's ends [3]. TB conductors have diameters ranging from 28.6 mm to 40.6 mm. Their ends are always fixed. A wind, when simulated, has a 13 m/s speed and a direction that is perpendicular to a conductor sample's longitudinal axis. It is called a side wind as any artificial wind movement is right to left in Fig. 1. That is, icing tends to form into the wind with a uniform longitudinal distribution.

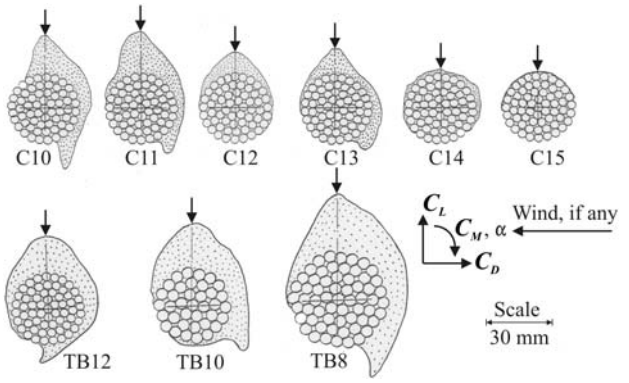

Fig. 1. Cross sections of transition ice growths. Arrows give zero wind incidence (α) for aerodynamic data.

Although the procedure of catching water droplets in oil to determine their MVD may be flawed [6], it permits a convenient check of a MVD's consistency and distinguishes clear differences. It gave the 1.5 mm and 1.0 mm MVD presented in Table I for the C and TB tests, respectively. Each value was virtually constant and a noticeable difference existed between the two values. The tabulated water droplets' terminal (vertical) speed was estimated by equating the aerodynamic drag on a spherical droplet with the droplet's weight. Drag coefficients were taken from Morsi and Alexander [7]; typical values were assumed otherwise [3]. It is noteworthy that a terminal speed should be attained well before a droplet reaches a conductor sample.

The air temperatures given in Table I are in a narrow range from about -3.0 °C to -1.5 °C. Therefore a 1 mm and 1.5 mm diameter (spherical) droplet is estimated [8] to have a temperature around -0.7 °C and 0 °C, respectively, at impact. A total (combined) precipitation amount, $H = \left(H_h^2 + H_v^2\right)^{1/2}$, shown in the table is back-calculated from the accreted ice weight [2]. The corresponding (combined) precipitation rate, P, is simply H divided by the total duration of a given experiment, t_{max}. Finally, G, the liquid water content (LWC) is determined from

$$G = \frac{P}{\beta V_T} \tag{1}$$

where

$$\beta = \sqrt{1 + \left(\frac{H_h}{H_v}\right)^2}\,. \tag{2}$$

The β is found empirically, by using the data of [2], to average 1.24 with about a -10% to +20% variation for a nominal 13 m/s side wind. Consequently β is taken pragmatically to be 1.24 (1) in the presence (absence) of the simulated wind. The V_T and P required in (1) are given in Table I together with the corresponding estimates of G. They are either low (C series) or at the high end of field data (TB series) [3]. The other environmental conditions appear realistic.

A replica of an iced conductor sample is obtained by first casting it in a Dow Corning® 3120 RTV silicone rubber which vulcanizes at room temperature. The procedure is similar to the one employed by Koutselos and Tunstall [9]. A permanent plaster of Paris model is made later around a central steel rod. Quasi-steady aerodynamic forces and moment acting on the replica are measured in a wind tunnel operating at room temperature. A replica is rotated automatically in π/90 rads (2°) increments so that the wind's angle of incidence, α, changes from 0 to 2 π rads. Coefficients of lift, drag and moment (C_L, C_D, and C_M respectively) are calculated conventionally and follow the sign convention shown in Fig. 1.

IV. Results

Aerodynamic coefficients measured at a free wind speed of 28 m/s are presented in Fig. 2 (a) for different α and H. This speed is noticeably higher than normally experienced in a natural freezing rainstorm [8]. However, the coefficients' derivatives with respect to the wind speed are quite flat between 15 m/s to 28 m/s. Below 15 m/s however, the wind tunnel's balance is relatively insensitive, especially for C_M. Corresponding empirically based predictions are given in Fig. 2 (b). They are derived from:

$$\left.\begin{aligned} C_L &= a_L b_L^{(1-\alpha/\pi)^2} \sin 3\alpha \\ C_M &= a_M b_M^{(1-\alpha/\pi)^2} \sin 2\alpha \\ C_D &= a_D + b_D \sin^2 \alpha \end{aligned}\right\} \tag{3}$$

for $0 \le \alpha \le 2\pi$. Coefficients a_i and b_i, i=L, M, D, are independent of α. Visual correlations with various environmental factors for the C series of conductors suggests that the coefficients are related primarily to H. These relationships are summarized in the second row of Table II.

TABLE I
CONDITIONS FOR TRANSITION ICE GROWTHS.

Conductor	Conductor diameter D_o (mm)	Wind/support condition	Nominal MVD d (mm)	Droplet's vertical collision speed V_T (m/s)	Air temperature (°C)	Combined precipitation H (mm)	Duration t_{max} (h)	Combined precipitation rate P (mm/h)	LWC G (g/m^3)
C10	28.6	WNR	1.5	5.5	-3.0	11.8	6	2.0	0.08
C11	28.6	WR	1.5	5.5	-3.0	12.3	6	2.1	0.08
C12	28.6	WR	1.5	5.5	-2.5	5.5	3	1.8	0.07
C13	28.6	WNR	1.5	5.5	-2.5	8.8	3	2.9	0.12
C14	28.6	NWR	1.5	5.5	-2.5	2.6	3	0.9	0.04
C15	28.6	NWNR	1.5	5.5	-2.5	0.1	3	0.0(3)	0.00(2)
TB8	40.6	WNR	1.0	4.0	-2.0	24.3	6	4.1	0.23
TB10	33.0	WNR	1.0	4.0	-1.5	23.2	4	5.8	0.32
TB12	28.6	WNR	1.0	4.0	-3.0	16.4	4	4.1	0.23

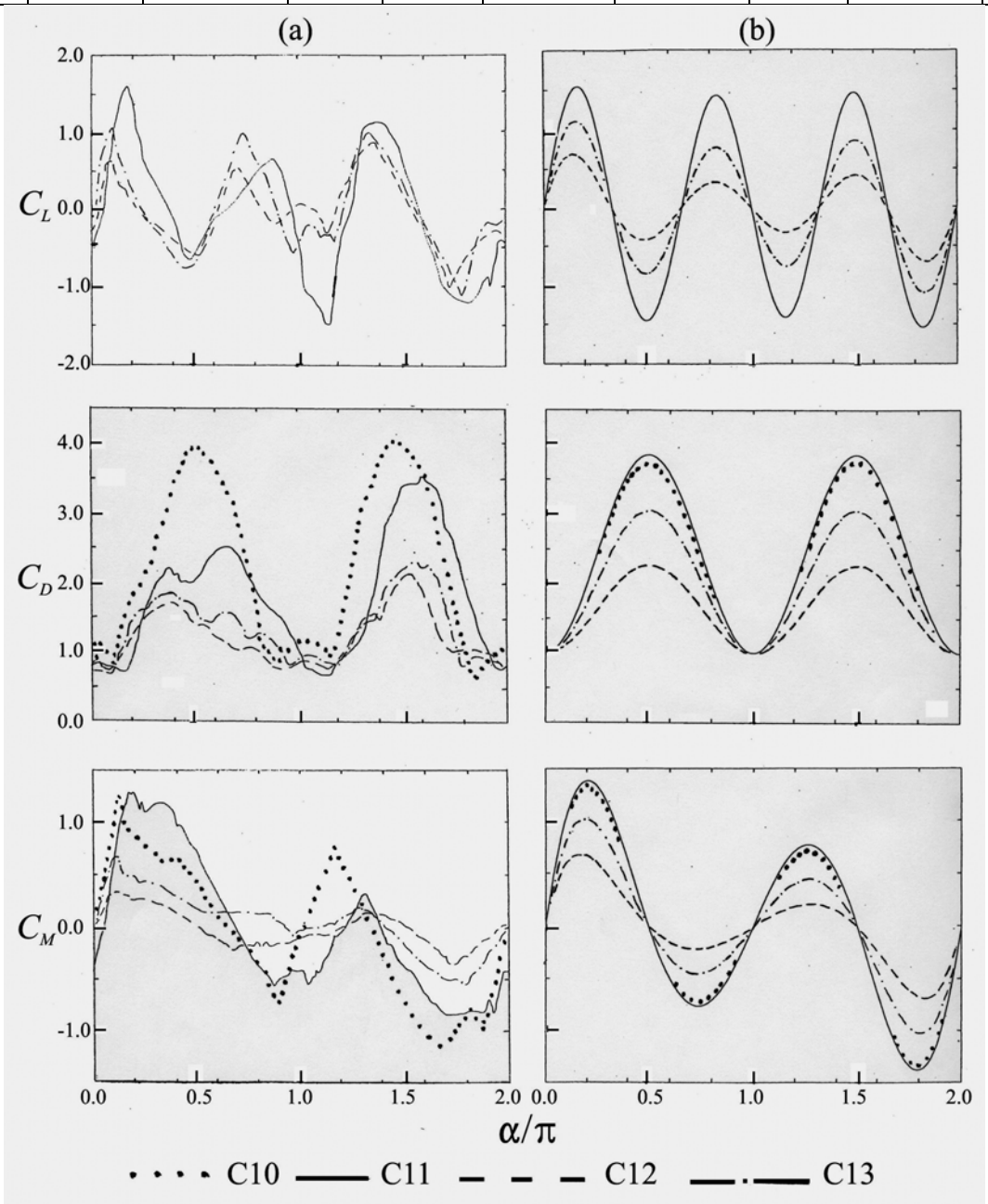

Fig. 2. Comparison of (a) measured and (b) predicted aerodynamic coefficients.

TABLE II
COEFFICIENT VALUES OF (3) AND CORRESPONDING AERODYNAMIC COEFFICIENTS AT SPECIFIED WIND INCIDENCES. *H* IS IN MM.

a_L	b_L	a_M	b_M	a_D	b_D
$0.013H^{1.87}$	$26H^{-1.25}$	$0.010H^{1.70}$	$70H^{-1.25}$	1	$0.232H$
$\|C_L\|$ at $\alpha=\pi/6, 11\pi/6$		$\|C_M\|$ at $\alpha=\pi/4, 7\pi/4$		C_D at $\alpha=\pi/2, 3\pi/2$	
$a_L b_L^{25/36} = 0.125H$		$a_M b_M^{9/16} = 0.109H$		$1+0.232H$	

Predictions agree fairly well with the overall measured behaviour for the C series of conductors. The measured data, however, is less smooth and it is not quite as asymmetrical for changes in α from α= π. The first discrepancy probably arises from occasional, relatively sharp local changes in the ice shapes illustrated in Fig. 1. The second discrepancy is the consequence of the substantially different ice accumulations (and, hence, shapes) above and below the conductors in this figure. This is especially true for C10 whose more prominent lower ice ridge generates noticeable variations but only in C_L and near α= π. This curve is shown separately in Fig. 3 to avoid obscuring the general trend in Fig. 2 (a).

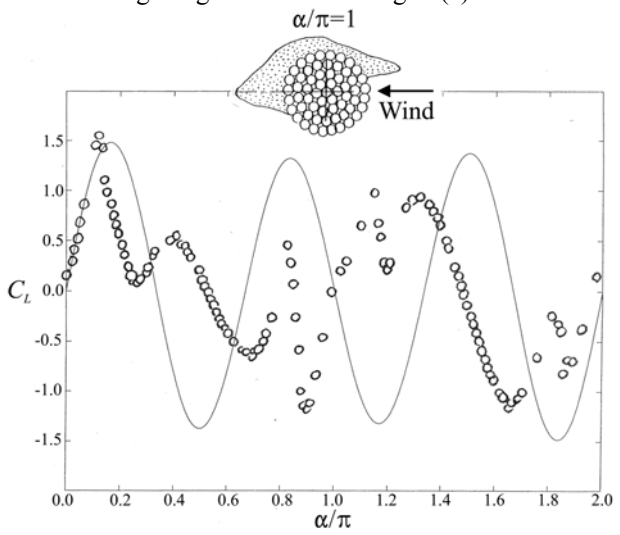

Fig. 3. Measurement (o) and prediction (-) of C_L for C10.

The maximax (over α) of the absolute aerodynamic coefficients have interest from a structural viewpoint. Such data can be found straightforwardly from plots like those given in Fig. 2. However, the task is simplified, but only for the predictions, by recognizing that the leftmost peak corresponds to the maximax value. Such predicted values can be found for the three aerodynamic coefficients from (3) and Table II. They are expressed analytically in terms of *H* in the fourth row of Table II. Fig. 4 shows the expressions as full lines in comparison to the discrete measurements. There is good agreement for the C conductors, including C10. All the maximax aerodynamic coefficients increase with *H* and the limited rotational capability appears to have little effect. (Compare, for example, C10 and C11.) However, the maximax C_D grow with *H* at about twice the rate or more of the other coefficients. Indeed it can be shown that the aerodynamic drag on C conductors having transition icing is significant, relative to the ice weight, even at low (sustained) wind speeds.

Aerodynamic measurements presented in Fig. 4 for TB12 suggest that, in comparison to the (same) 28.6 mm diameter C conductors, water droplets having a smaller MVD appear to reduce the maximax aerodynamic values at larger *H*. On the other hand, the maximax $|C_L|$ and C_D are little different for the 33.0 mm (TB10) and 40.6 mm (TB8) conductor diameters. Hence, the conductor diameter may be relatively unimportant for a given MVD. If so, a smaller MVD for the droplets seems to more universally generate lower aerodynamic curves, with increasing *H*.

V. CONCLUSIONS

Many visual observations of conductor icing indicate a need to introduce a third growth category (transition icing) to adequately represent different ice shapes (with associated surface textures) and their aerodynamic behaviour. The preliminary assessment of the modest transition icings presented here suggests that aerodynamic trends may be reasonably predicted for a given power line surprisingly simply from environmental properties.

VI. ACKNOWLEDGMENTS

The interactions and aid over many years from colleagues and students is appreciated. The most notable individuals are Dr. J. Tinkler and Mr. W. Barrett, both unfortunately deceased now, Dr. A.H. Shah, Brent Naherny, Peter Stumpf, Henry Ng and Kent Seguin. Abdu Mahmoud and Darryl Stoyko helped to prepare this paper. The financial contributions of the Natural Science and Engineering Research Council of Canada (NSERC), Manitoba Hydro and the Canadian Electrical Association (CEA) are acknowledged gratefully.

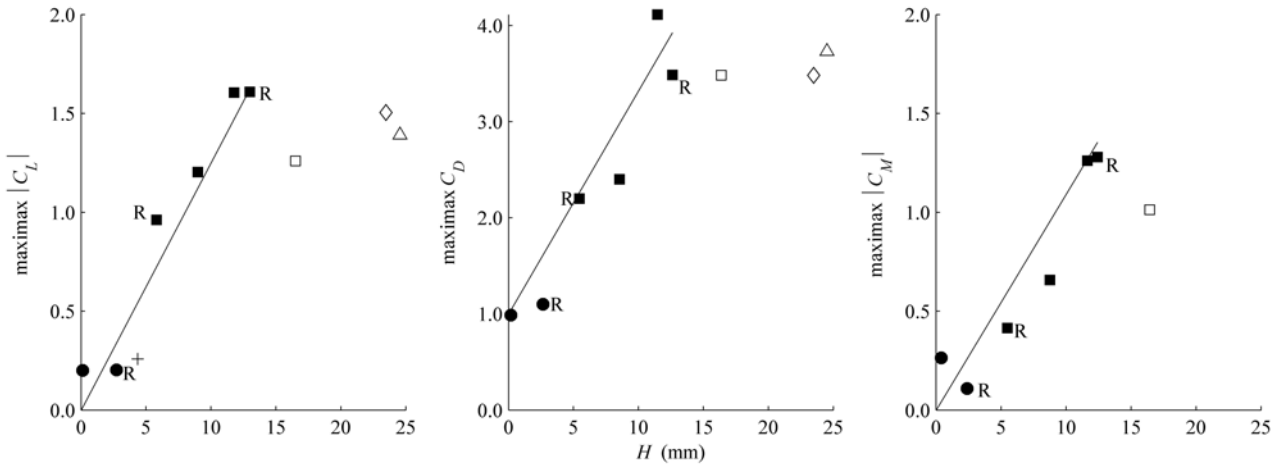

Measurements

Predictions using Table II

d (mm)	D_o (mm)			
	28.6		33.0	40.6
1.0		□ (TB12)	◇ (TB10)	△ (TB8)
1.5	●	■		
	NW	W		

+ Conductor sample is fixed if R (rotation permitted) is omitted.

Fig. 4. Maximax aerodynamic data.

VII. References

[1] J. Tinkler, N. Popplewell, and A.H. Shah, "Effects of freezing rain on guyed towers," presented at the Int. Conf. on Flow Induced Vibrations, Bowness-on-Windermere, England, 1987, pp. 575-583.

[2] M.L. Lu, N. Popplewell, and A.H. Shah, "Freezing rain simulations for fixed, unheated conductor samples," *J. App. Meteorology*, vol 39 (12), pp. 2385-2396, 2000.

[3] G. Poots, *Ice and snow accretion on structures*, New York: Wiley, 1996.

[4] P. Stumpf and H.C.M. Ng, "Investigation of aerodynamic stability for selected inclined cables and conductor cables," B.Sc. thesis, Dept. Mech. Eng., Univ. Manitoba, 1990.

[5] K. Seguin, "Wind tunnel testing of iced cable models," B.Sc. thesis, Dept. Mech. Eng., Univ. Manitoba, 1995.

[6] K.J. Finstad, "Transmission line icing model," Ph.D. dissertation, Dept. Geog., Univ. Alberta, 1989.

[7] S.A. Morsi, and A.J. Alexander, "Collision efficiency of a particle with a sphere and a cylinder," presented at the Int. Conf. on Pneumatic Transport of Solids in Pipes, Cambridge, England, 1971.

[8] B. Naherny, "Further study of iced-conductor cable generation by using a freezing rain simulator," B.Sc. thesis, Dept. Mech. Eng., Univ. Manitoba, 1990.

[9] L.T. Koutselos, and M.J. Tunstall, "Collection and reproduction of natural ice shapes on overhead line conductors and measurement of their aerodynamic characteristics," in Proc. 1986 3rd. IWAIS, Vancouver, Canada, 1986.